Terminal Control of a Gliding Parachute in a Nonuniform Wind

A. E. Pearson,* K. C. Wei,† and R. M. Koopersmith†
Brown University, Providence, R.I.

Least squares estimation and an open-loop control based on geometric considerations are combined to define a closed-loop terminal control law for a gliding parachute system under variable wind conditions. Closed-form solutions are obtained for the analysis of the nonlinear kinematic equations of motion. Simulation results of the overall system are included for a variety of initial conditions and wind profiles.

I. Introduction

INTEREST in the guidance and control of a gliding parachute system has developed in recent years in connection with payload recovery for sounding-rocket flights[1] and cargo delivery for air transport vehicles.[2] The Para-Foil[3] and Para-Wing are two examples of such gliding systems in which control is effected by a servomotor connected to the suspension lines of the parachute. Electronic signals from a ground based transmitter command rotations of the motor which cause the parachute to execute a right or left banked turn in relation to the difference in pull on the right and left suspension lines. Radial homing has been utilized in several applications[1,3] as an easily implemented control law to reduce terminal missed distance from a given target at touchdown. Referring to Fig. 1 where $\boldsymbol{p}$ is the position vector of the parachute relative to a fixed target in the horizontal plane, v is the horizontal component of the velocity vector of the parachute relative to air, and $\boldsymbol{w}$ is the wind velocity vector, the radial homing control law attempts to align v with $-\boldsymbol{p}$, i.e., to keep the angle γ near zero at all times. The angular error γ is sensed by a pair of directional antennas on board the parachute which receive signals from a gound based transmitter. However, theoretical analyses,[4-7] together with flight test results,[1,3] indicate that the terminal accuracy of radial homing is sensitive to deviations from an appropriate launch area, which depends on the wind and altitude, as well as the effects of a nonuniform wind.

In this paper, an alternative control law is developed which combines wind estimation and an open-loop control based on geometric considerations for the terminal control of a gliding parachute is a nonuniform wind. Following a statement of the problem in Sec. II, a least squares estimation for the wind and initial heading is considered in Sec. III, while the open-loop control is given in Sec. IV together with a discussion of an optimal control which has some interesting features. Simulation results of the closed loop control law are given in Sec. V.

II. Problem Statement

It will be assumed that control is initiated after full deployment of the parachute has occurred, that the speed of the parachute relative to wind is a known constant, that the descent rate is constant, and that the vertical component of the wind vector is negligible in relation to the horizontal component. Then the equations of motion of the center of mass can be written as

$$\dot{p}_1(t) = a\cos\theta(t) + w_1(t) \tag{1a}$$

$$\dot{p}_2(t) = a\sin\theta(t) + w_2(t) \quad 0 \le t \le T \tag{1b}$$

$$\dot{\theta}(t) = (g/a)\tan\phi(t) \tag{1c}$$

where $[p_1(t), p_2(t)]$ denote the position coordinates of the parachute in the horizontal plane relative to the target, $[w_1(t), w_2(t)]$ are the velocity components of the wind vector, $\theta(t)$ is the instantaneous heading of the parachute velocity vector relative to air, and $\phi(t)$ is the parachute bank angle relative to the local vertical. The speed of the parachute in the horizontal plane relative to air is denoted by the constant a which is presumed to be of sufficient magnitude to facilitate a wind penetration capability; T is the time to go until touchdown from the initial deployment time zero. Alternatively, Eq. (1c) can be expressed in terms of the instantaneous radius of turn, $r(t)$, of the parachute in the horizontal plane via the well known kinematic relation

$$\tan\phi = a^2/gr \tag{2a}$$

i.e.

$$\dot{\theta}(t) = a/r(t) \tag{2b}$$

The control objective is to choose the proper bank angle $\phi(t)$ over $0 \le t \le T$, via appropriate rotations in the servomotor, such that the parachute lands as close to the target as possible at the terminal time T, and that the heading of the parachute be upwind at the terminal time in order to minimize the total speed of the parachute at impact. Thus, ideally, the desired terminal conditions are

$$p_1(t) = p_2(T) = 0, \quad \theta(t) = \underline{/W(T)} \pm \pi \tag{3}$$

where $\underline{/W(T)}$ denotes the wind direction at the terminal time. The approach of this paper is to regard $\phi(t)$ as the control variable, thus neglecting the actuator dynamics of the servomotor, and to separate the estimation and control problems over successive time intervals in a step-by-step control-estimation sequence. In this regard, let the time interval $0 \le t \le T$ be divided into N nonoverlapping subintervals $t_i \le t \le t_{i+1}$, $i = 0,1 \ldots N-1$, with $t_0 = 0$ and $t_N = T$. The estimation problem relative to the ith subinterval, $t_i \le t \le t_{i+1}$, consists of estimating the initial heading, $\theta(t_i)$, and the wind profile $w(t)$ over $t_i \le t \le T$, based on observed data collected over the previous subinterval or intervals. The observed data

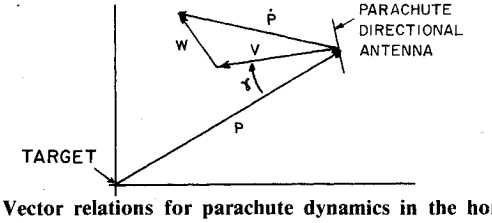

Fig. 1 Vector relations for parachute dynamics in the horizontal plane.

Received Dec. 13, 1976; revision received March 21, 1977.
Index categories: Guidance and Control; Deceleration Systems.

*Professor of Engineering. Division of Engineering and Lefschetz Center for Dynamical System.
†Graduate Student Research Assistant. Division of Engineering and Lefschetz Center for Dynamical System.

is assumed to be comprised of the parachute bank angle $\phi(t)$, the position vector $p(t)$, and possibly (depending on the estimation scheme) the total velocity vector of the parachute $\dot{p}(t)$. Given the estimates $\hat{\theta}(t_i)$ and $\hat{w}(t)$ for $t_i \le t \le T$, the control problem relative to the ith subinterval consists of choosing the bank angle $\phi(t)$, or equivalently the turning radius $r(t)$, on $t_i \le t \le t_{i+1}$ such that the parachute would land as close to the target as possible in an upward wind direction at the terminal time if, in fact, the estimates $\hat{\theta}(t_i)$ and $\hat{w}(t)$ were exact and $\phi(t)$ were applied for all t in the interval $t_i \le t \le T$. The estimates $[\hat{\theta}, \hat{w}(\cdot)]$ are updated over the next subinterval based on the new data collected over that interval, and similarly the control variable $\phi(t)$ is recomputed based on the new estimates, resulting in a step-by-step control-estimation sequence which constitutes the closed-loop control algorithm. Although there are no hard constraints on the bank angle $\phi(t)$, it is desirable to keep $|\phi|$ within reasonable limits of approximately 30°.

In the following sections, a computationally feasible solution is presented to the above problem which utilizes a least squares estimation and a control based on geometric considerations.

III. Wind and Initial Heading Estimation

Let $t_0 \le t \le t_1$ be a typical subinterval over which data is observed and it is desired to obtain estimates of the wind profile $w(t)$ and initial heading angle $\theta(t_0) = \theta_0$ for purpose of updating the control algorithm on the next subinterval. The wind components in Eqs. (1) will be modeled by the polynomials of preselected order n:

$$w_1(t) = \sum_{i=0}^{n} \alpha_i t^i \tag{4a}$$

$$w_2(t) = \sum_{i=0}^{n} \beta_i t^i \tag{4b}$$

In practical terms n would probably be chosen as either $n=0$ (a constant wind of unknown magnitude and direction), or $n=1$ (a variable wind with linear time varying components). A least squares estimate of the parameters $(\theta_0, \alpha_0 .. \alpha_n \beta_0 \ldots \beta_n)$ results upon minimizing the functional

$$J(\theta_0,\alpha,\beta) = \int_{t_0}^{t_1} [\dot{p}_1(t) - a\cos[\theta_0 + U(t)] - \sum_{i=0}^{n} \alpha_i t^i]^2 dt + \int_{t_0}^{t_1} [\dot{p}_2(t) - a\sin[\theta_0 + U(t)] - \sum_{i=0}^{n} \beta_i t^i]^2 dt \tag{5}$$

where $U(t)$ is defined in terms of the bank angle $\phi(t)$ by

$$U(t) = \frac{g}{a} \int_{t_0}^{t} \tan\phi(\tau)\, d\tau$$

A necessary condition for the minimization of Eq. (5) is the adherence of the following relations:

$$\frac{\partial J}{\partial \theta_0} = 0, \quad \frac{\partial J}{\partial \alpha_i} = 0, \quad \frac{\partial J}{\partial \beta_i} = 0 \quad i = 0,1..n \tag{6}$$

Since J is quadratic in the α_i and β_i parameters, the second and third sets of equations in Eq. (6) are linear in (α,β) and can be solved uniquely for (α,β) in terms of θ_0 and the data. The coefficient matrix for the linear equations in (α,β) is the Gramian for the functions $\{1, t \cdots t^n\}$ on $t_0 \le t \le t_1$, i.e., the symmetric matrix whose ijth component ($i=0. \ldots n$ and $j=0 \ldots n$) is defined by

$$G_{ij} = \int_{t_0}^{t_1} t^{i+j} dt = \frac{t_1^{i+j+1} - t_0^{i+j+1}}{i+j+1}, \quad 0 \le i,j \le n \tag{7}$$

Since $\{1, t \ldots t^n\}$ are linearly independent for any $t_1 > t_0$, the inverse matrix of G exists and can be precomputed and stored for any given $t_0 \le t \le t_1$ interval. Letting H_{ij} denote the ijth component of the inverse matrix, G^{-1}, the solutions for α_i and β_i become (details omitted):

$$\alpha_i = \sum_{j=0}^{n} H_{ij}[X_j - a(C_j\cos\theta_0 - S_j\sin\theta_0)] \tag{8a}$$

$$0 \le i \le n$$

$$\beta_i = \sum_{j=0}^{n} H_{ij}[Y_j - a(C_j\sin\theta_0 + S_j\cos\theta_0)] \tag{8b}$$

where the scalars (C_j, S_j, X_j, Y_j) are given by

$$C_j = \int_{t_0}^{t_1} t^j \cos U(t)\, dt, \quad S_j = \int_{t_0}^{t_1} t^j \sin U(t)\, dt \tag{9}$$

$$X_j = \int_{t_0}^{t_1} t^j \dot{p}_1(t)\, dt, \quad Y_j = \int_{t_0}^{t_1} t^j \dot{p}_2(t)\, dt \tag{10}$$

Substituting Eq. (8) into the first of the relations in Eq. (6) leads to the result

$$\partial J/\partial\theta_0 = 0 = A\sin\theta_0 - B\cos\theta_0 \tag{11}$$

where A and B are defined by

$$A = \int_{t_0}^{t_1} [\dot{p}_1(t)\cos U(t) + \dot{p}_2(t)\sin U(t)]dt - \sum_{i=0}^{n}\sum_{j=0}^{n} H_{ij}[X_jC_i + Y_jS_i] \tag{12}$$

and

$$B = \int_{t_0}^{t_1} [\dot{p}_2(t)\cos U(t) - \dot{p}_1(t)\sin U(t)]dt + \sum_{i=0}^{n}\sum_{j=0}^{n} H_{ij}[X_jS_i - Y_jC_i] \tag{13}$$

respectively. Assuming the bank angle $\phi(t)$ is not identically zero on $t_0 \le t \le t_1$, or equivalently that $U(t)$ is not identically zero, Eq. (11) can be solved for θ_0, modulo 2π, taking into account that a minimal value is desired, i.e., taking note of the condition that $\partial^2 J/\partial\theta_0^2 > 0$. This solution is given by

$$\hat{\theta}_0 = 2m\pi + \tan^{-1}(B/A) \tag{14}$$

where m is any integer. Substituting Eq. (14) into Eq. (8) then yields the final closed-form solution for the least squares estimate of the quantities (θ_0,α,β).

The previous solution is contingent on the condition that $\phi(t) \not\equiv 0$ because A and B each vanish if $\phi(t) = 0$ on $t_0 \le t \le t_1$. In the event that $\phi(t) = 0$ for all t on $t_0 \le t \le t_1$, θ_0 cannot be estimated from the given data. In this case a prior value for θ_0 should be assumed, based on data collected over a previous subinterval in which $\phi(t) \not\equiv 0$, and $(\hat{\alpha},\hat{\beta})$ can be obtained from

$$\hat{\alpha}_i = \sum_{j=0}^{n} H_{ij}(X_j - aG_{j0}\cos\hat{\theta}_0) \tag{15a}$$

$$\hat{\beta}_i = \sum_{j=0}^{n} H_{ij}(Y_j - aG_{j0}\sin\hat{\theta}_0) \tag{15b}$$

where $\hat{\theta}_0$ is the a priori value assumed for θ_0.

Finally, it should be noted that the integrals involving the total velocity vector of the parachute, $\dot{p}(t)$, in Eqs. (10, 12,

and 13) can be equivalently expressed in terms of $p(t)$ using integration by parts, i.e.,

$$X_j = t_1{}^j p_1(t_1) - t_0{}^j p_1(t_0) - j\int_{t_0}^{t_1} t^{j-1} p_1(t)\,dt \tag{16a}$$

$$Y_j = t_1{}^j p_2(t_1) - t_0{}^j p_2(t_0) - j\int_{t_0}^{t_1} t^{j-1} p_2(t)\,dt \tag{16b}$$

$$\int_{t_0}^{t_1} \dot{p}_i(t)\cos U(t)\,dt = p_i(t_1)\cos U(t_1) - p_i(t_0) + \frac{g}{a}\int_{t_0}^{t_1} p_i(t)\tan\phi(t)\sin U(t)\,dt \tag{17a}$$

$$i=1,2$$

$$\int_{t_0}^{t_1} \dot{p}_i(t)\sin U(t)\,dt = p_i(t_1)\sin U(t_1) - \frac{g}{a}\int_{t_0}^{t_1} p_i(t)\tan\phi(t)\cos U(t)\,dt \tag{17b}$$

Thus, a knowledge of the data $[p(t), \phi(t)]$ on $t_0 \le t \le t_1$ is sufficient to obtain the least squares estimate of the wind model, Eq. (4), and initial heading $\theta(t_0)$.

If a more elaborate statistical estimate is sought for the pair $[\theta_0, w(\cdot)]$, it is possible to formulate a recursive scheme utilizing Kalman-Bucy filtering techniques, assuming the wind vector has a randomly varying direction but a constant magnitude value, and assuming the total velocity vector of the parachute, $\dot{p}(t)$, is available, corrupted by white-noise Gaussian processes.[11] However, the computations are significantly more complex as discussed in Ref. 11, including nonlinear transformations on the data, and hence the aforementioned least squares estimate will be used here.

IV. The Terminal Control Problem

Given estimates of the wind vector $w(t)$ over $t_0 \le t \le T$ and the initial heading of the parachute relative to wind, $\theta(t_0)$, as discussed in Sec. III, the following transformations to normalized coordinates simplify the dynamic equations for control considerations:

$$x_i(t) = \frac{1}{(T-t_0)a}\left[p_i(t) + \int_t^T w_i(\xi)\,d\xi\right], \quad i=1,2 \tag{18a}$$

$$x_3(t) = \theta(t) \tag{18b}$$

Rewriting Eq. (1) in terms of (x_1, x_2, x_3) and introducing the normalized time τ,

$$\tau = (t-t_0)/(T-t_0) \tag{19}$$

and the normalized control variable u,

$$u = [(T-t_0)g/a]\tan\phi \tag{20}$$

the kinematic equations become

$$\dot{x}_1(\tau) = \cos x_3(\tau) \tag{21a}$$

$$\dot{x}_2(\tau) = \sin x_3(\tau) \qquad 0 \le \tau \le 1 \tag{21b}$$

$$\dot{x}_3(\tau) = u(\tau) \tag{21c}$$

The desired terminal state in these coordinates is given by:

$$x_1(1) = x_2(1) = 0, \quad x_3(1) = \underline{/w(T)} + \pi \tag{22}$$

where $\underline{/w(T)}$ denotes the estimated wind direction at the terminal time T.

The following general observations for any control u, optimal or otherwise, are evident from Eq. (21):

1) The speed of the parachute in the $x_1 - x_2$ plane is unity since an element of arc length is $ds = (x_1^2 + x_2^2)^{1/2}$ and the speed is

$$ds/d\tau = [(x_1)^2 + (x_2)^2]^{1/2} = [\cos^2 x_3 + \sin^2 x_3]^{1/2} = 1$$

Thus a trajectory over $0 \le \tau \le 1$ must have unit length and, moreover, it is necessary that the initial conditions, $x_1(0)$ and $x_2(0)$, lie inside the unit circle in order to achieve the ideal terminal state, Eq. (22).

2) The control $-u(\tau)$ results in a trajectory which is the mirror image about the x_1 axis of the trajectory given by $+u(\tau)$.

Observation (1) facilitates a simple geometric solution to the terminal control problem for the case in which the initial conditions $[x_1(0), x_2(0)]$ lie inside the unit circle, as well as suggests a reasonable control strategy when the initial conditions $[x_1(0), x_2(0)]$ lie on or outside the unit circle. These solutions are presented in the following sections.

A. Control for Initial Conditions Inside the Unit Circle

Referring to Fig. 2a, the simplest continuous path that satisfies the terminal constraints, Eq. (22), when the initial conditions $[x_1(0), x_2(0)]$ lie inside the unit circle consists of two circular arcs of equal radius separated by a straight line. The corresponding control for this path is shown in Fig. 2b where ρ is the normalized radius of curvature of the parachute in the horizontal plane. Since three parameters characterize this path (ρ, τ_1, τ_2) it can be expected that a solution exists for these parameters which satisfy the terminal constraints of Eq. (22) given the initial data $[x_1(0), x_2(0), x_3(0)]$. In this connection a control law is considered of the form

$$u(\tau) = \begin{cases} \rho^{-1}, & 0 \le \tau < \tau_1 \\ 0, & \tau_1 \le \tau \le \tau_2 \\ \rho^{-1}, & \tau_2 < \tau \le 1 \end{cases} \tag{23}$$

where ρ can be either positive or negative, depending on the counter clockwise or clockwise traversal of the circular arcs in Fig. 2a.

Integrating the differential equations, (21), using the control equation, (23), and incorporating the terminal constraints, (22), the resulting algebraic equations can be solved for (ρ, τ_1, τ_2) in terms of the given data $[x_1(0), x_2(0), x_3(0)]$. This nonunique, but closed-form solution is summarized by the following relations which depend on an arbitrary integer n arising from the modulo 2π condition of the terminal constraint on the angle x_3: given

$$[x_1(0), x_2(0), x_3(0)] \text{ with } x_1^2(0) + x_2^2(0) < 1,$$

define ψ_n by

$$\psi_n = 2n\pi - x_3(0), \quad n = 0, \pm 1, \ldots \tag{24}$$

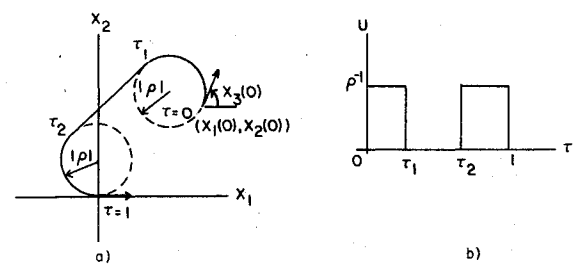

Fig. 2 Trajectory based on geometrical considerations.

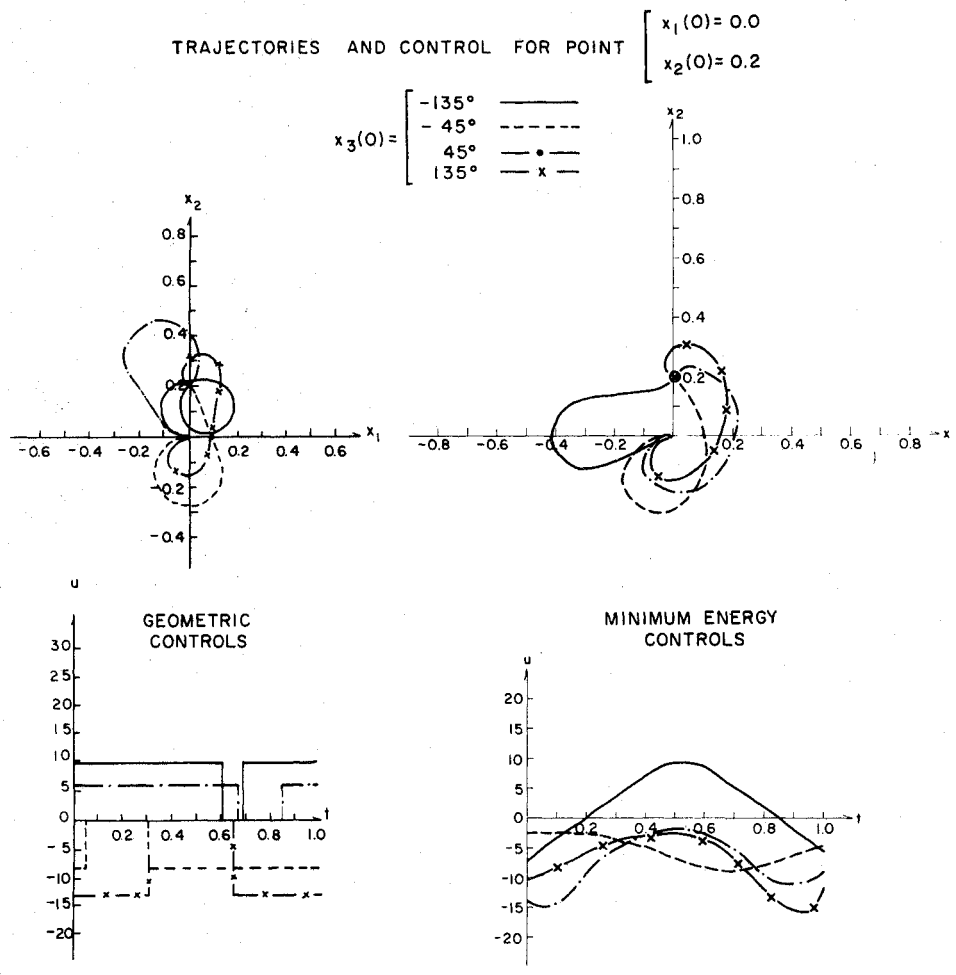

Fig. 3 Comparison of geometric and minimum energy controls.

and form (a_n, b_n, c_n) from the expressions

$$a_n = \psi_n^2 - 2[1 - \cos x_3(0)] \tag{25a}$$

$$b_n = \psi_n \dot{-} x_2(0)[1 - \cos x_3(0)] - x_1(0)\sin x_3(0) \tag{25b}$$

$$c_n = 1 - x_1^2(0) - x_2^2(0) \tag{25c}$$

Then the turning radius ρ_n, parameterized by the integer n, is given nonuniquely by

$$\rho_n = a_n^{-1}[b_n \pm (b_n^2 - a_n c_n)^{1/2}] \tag{26}$$

and the switching times (τ_1, τ_2) by

$$\tau_1(n) = \rho_n(\omega_n - x_3(0)) \tag{27a}$$

$$\tau_2(n) = 1 - \rho_n(2n\pi - \omega_n) \tag{27b}$$

where the angle ω_n is obtained (unique to within arbitrary multiples of 2π) from the pair of equations

$$\cos\omega_n = (1 - \rho_n\psi_n)^{-1}[\rho_n \sin x_3(0) - x_1(0)] \tag{28a}$$

$$\sin\omega_n = (1 - \rho_n\psi_n)^{-1}\{\rho_n[1 - \cos x_3(0)] - x_2(0)\} \tag{28b}$$

The derivation of Eqs. (24-28), together with a Fortran program which enumerates all physically acceptable trajectories‡ is given in Sec. VI of Ref. 9. Nonuniqueness among physically acceptable trajectories is resolved by selecting that value of n which leads to the largest $|\rho_n|$ i.e. least control effort on $0 \le \tau \le 1$. Computer simulations summarized in Ref. 9 indicate that the largest $|\rho_n|$ corresponds to a value of n in the set $\{-1,0,1\}$, at least among all initial conditions tested.

It might be supposed that a modification of the control, Eq. (23), which allows for traversals of the circular arcs in opposite sense from one another would also lead to a computationally feasible solution, i.e., modifying the lower portion of Eq. (23) to $u(\tau) = -\rho^{-1}$ for $\tau_2 < \tau \le 1$. However, the algebraic equations arising from the terminal constraints, Eq. (22), cannot be solved in closed form for (ρ, τ_1, τ_2) in terms of $[x_1(0), x_2(0), x_3(0)]$ as in the case of the solution for Eq. (23). Hence, this case is not considered further even though its solution might lead to larger turning radii (smaller control effort) than the previous solution for particular initial data.

B. Control for Initial Conditions Outside the Unit Circle

Consider the following control strategy for the case in which $[x_1(0), x_2(0)]$ lie outside the unit circle. Let $u(\tau)$ be constrained to be either one of the two forms:

$$u_1(\tau) = \begin{cases} \rho^{-1} & \text{for } 0 \le \tau \le \tau_1 \\ 0 & \text{for } \tau_1 < \tau \le 1 \end{cases} \tag{29}$$

or

$$u_2(\tau) = \begin{cases} 0 & \text{for } 0 \le \tau \le \tau_1 \\ \rho^{-1} & \text{for } \tau_1 < \tau \le 1 \end{cases} \tag{30}$$

where the normalized turning radius, ρ, and the switching time τ_1 are to be determined by minimizing the function

$$J(\tau_1) = [x_1^2(1) + x_2^2(1)] \tag{31}$$

‡A physically acceptable trajectory is a solution for which ρ_n is real and $0 \le \tau_1(n) \le \tau_2(n) \le 1$.

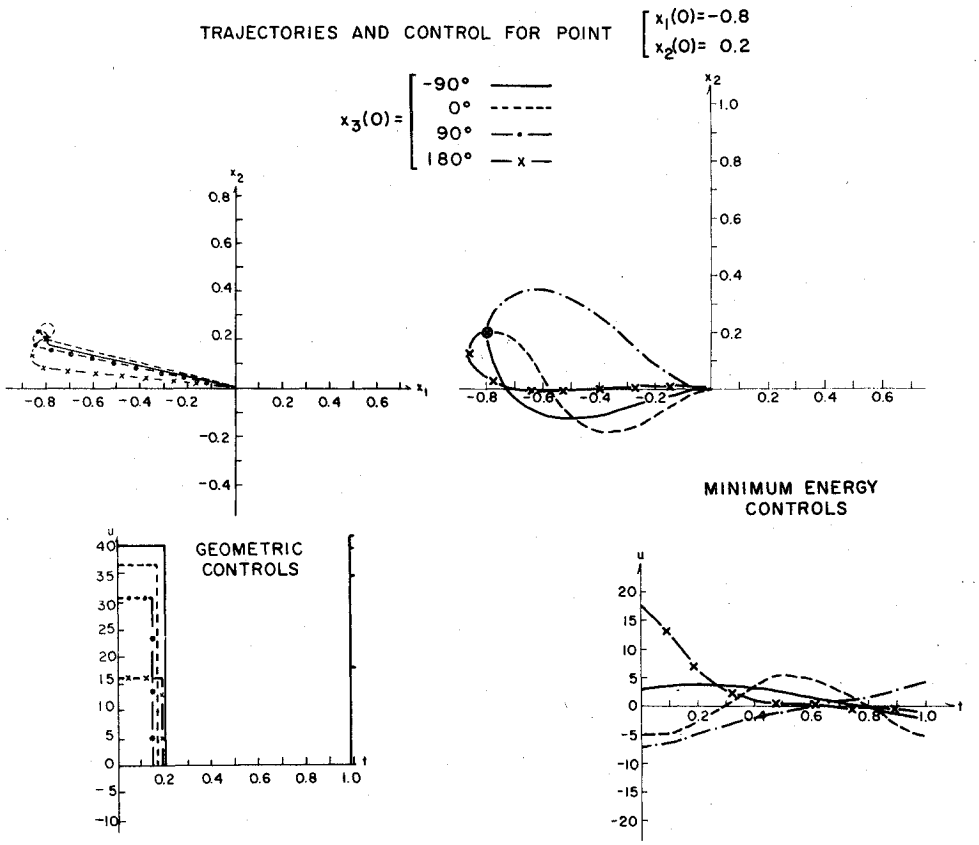

Fig. 4 Comparison of geometric and minimum energy controls.

subject to the end-point constraint

$$x_3(1) = \underline{/w(T)} + \pi \tag{32}$$

Using the control u_1 in Eq. (29), the equations of motion, Eqs. (21), can be integrated yielding an explicit expression for $J(\tau_1)$. The terminal constraint, Eq. (32), implies the following relation between ρ and τ_1:

$$\rho = \tau_1 / [\underline{/w(T)} + \pi - x_3(0)] \tag{33}$$

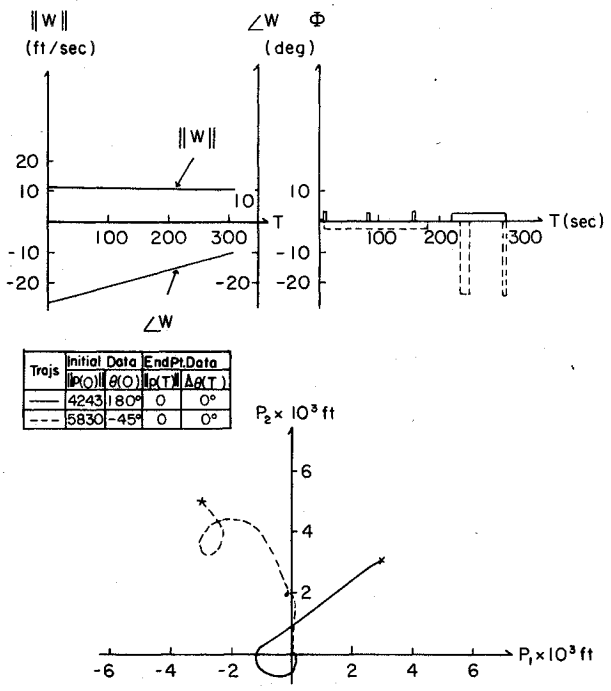

Fig. 5 Simulation data for closed-loop control.

Using this constraint and the necessary condition for a minimum, $dJ/d\tau_1 = 0$, the following values for τ_1^* and $J^* = J(\tau_1^*)$ are obtained:

$$\tau_1^* = \frac{1}{d}\Big(1 + x_1(0)\cos\nu + x_2(0)\sin\nu + \frac{1}{x_3(0)-\nu}\{x_1(0)\sin\nu - x_2(0)\cos\nu - x_1(0)\sin x_3(0) + x_2(0)\cos x_3(0) + \sin[\nu - x_3(0)]\}\Big) \tag{34}$$

$$J_1^* = \frac{1}{d}\Big\{x_2(0)\cos\nu - x_1(0)\sin\nu + \frac{1}{\nu - x_3(0)}\{x_1(0)\cos x_3(0) + x_2(0)\sin x_3(0) + \cos[\nu - x_3(0)] - 1 - x_1(0)\cos\nu - x_2(0)\sin\nu\}\Big\}^2 \tag{35}$$

where d and ν are defined by

$$\nu = \underline{/w(T)} + \pi \tag{36}$$

$$d = \frac{\{\nu - x_3(0) - \sin[\nu - x_3(0)]\}^2 + 4\sin^4\left(\frac{\nu - x_3(0)}{2}\right)}{[\nu - x_3(0)]^2} \tag{37}$$

With the previously defined value for τ_1^*, it can be shown that $d^2J/d\tau_1^2 > 0$ so that τ_1^* is a minimal point. This implies that u_1 in Eq. (29) will be the proper control to apply (within the present context) provided, in addition, that $0 \le \tau_1^* \le 1$ and $\nu \ne x_3(0)$.

In a similar manner, the differential equations can be integrated using the control u_2 in Eq. (30) resulting in an explicit relation for $J(\tau_1)$. Again, the terminal constraint, Eq. (32), implies the following constraint between the radius of turn ρ

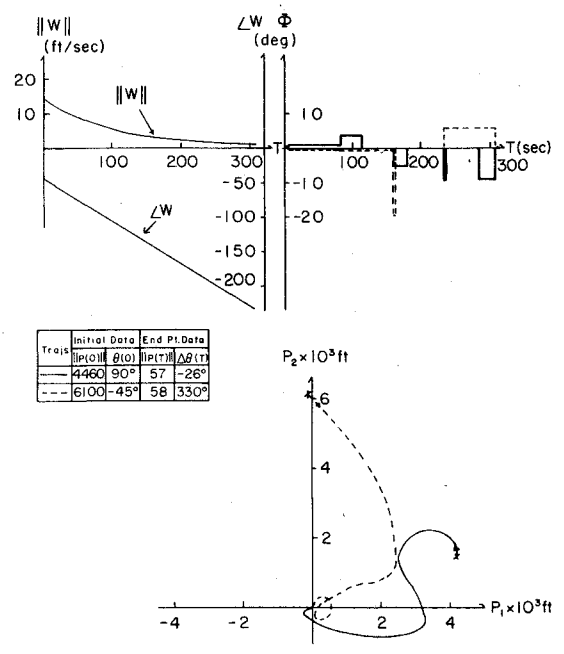

Trajs	Initial Data ‖P(0)‖	θ(0)	End Pt. Data ‖P(T)‖	Δθ(T)
——	4460	90°	57	-26°
- - -	6100	-45°	58	330°

Fig. 6 Simulation data for closed-loop control.

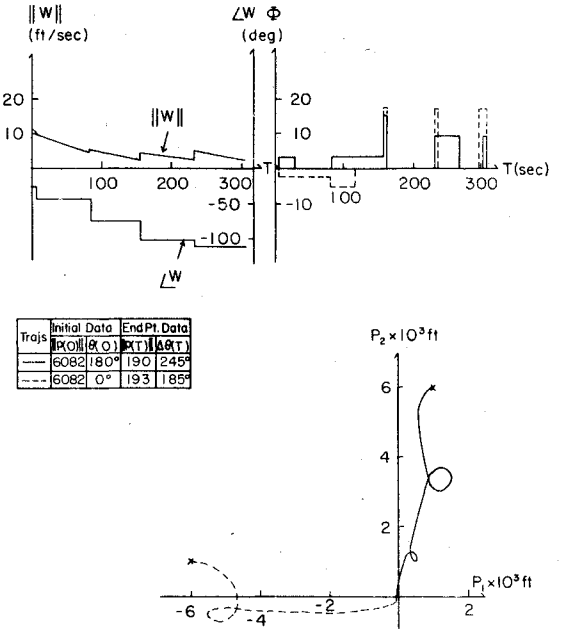

Trajs	Initial Data ‖P(0)‖	θ(0)	End Pt. Data ‖P(T)‖	Δθ(T)
——	6082	180°	190	245°
- - -	6082	0°	193	185°

Fig. 7 Simulation data for closed-loop control.

and τ_1 [cf. Eq. (33)]:

$$\rho = \frac{1-\tau_1}{|w(T) + \pi - x_3(0)} \tag{38}$$

The minimizing value of τ_1 and corresponding minimal value of J in this case is found to be

$$\tau_1^* = \frac{1}{d}\left(\frac{2-2\cos(\nu - x_3(0))}{[\nu - x_3(0)]^2} + \frac{1}{\nu - x_3(0)} \{ x_1(0)\sin\nu - x_2(0)\cos\nu + x_2(0)\cos x_3(0) - x_1(0)\sin x_3(0) - \sin[\nu - x_3(0)]\} - x_1(0)\cos x_3(0) - x_2(0)\sin x_3(0) \right) \tag{39}$$

and

$$J_2^* = \frac{1}{d}\Big\{ x_1(0)\sin x_3(0) - x_2(0)\cos x_3(0) + \frac{1}{\nu - x_3(0)} \{ x_1(0)\cos\nu + x_2(0)\sin\nu - x_1(0)\cos x_3(0) - x_2(0)\sin x_3(0) - 1 + \cos[\nu - x_3(0)]\} \Big\}^2 \tag{40}$$

As in the previous case, u_2 is feasible only if τ_1^* in Eq. (39) satisfies $0 \le \tau_1^* \le 1$. In practice, both cases must be considered for any particular set of initial values $[x_1(0), x_2(0)]$ lying outside the unit circle with the choice, u_1 or u_2, based on feasibility. It could be that neither case is feasible for certain initial data in which case the value of J can be computed for full on, or full off, control during $0 \le \tau \le 1$, and that control selected which achieves the smaller value for J, consistent with the end-point heading constraint, Eq. (32). These details of the control strategy have been programmed into the Fortran listing supplied in the Appendix of Ref. 11.

C. Optimal Controls

The controls discussed in subsections A and B are optimal within the context of the constraints imposed on the form of the control signals, Eqs. (23, 29, and 30), and the end-point constraints. However, minimum energy controls without the piecewise constant constraint can potentially offer solutions with less control effort for the same terminal accuracy. Several versions of minimum energy control problems have been examined in Refs. 8-10. Assuming the initial data $[x_1(0), x_2(0)]$ within the unit circle so that the ideal terminal constraints, Eq. (22), can be employed, the optimal control u^* which minimizes $J(u) = \int_0^t u^2(\tau)\,d\tau$ subject to Eqs. (21-22) has the interesting property that it is linear in the (x_1, x_2) states (see Sec. III of Ref. 9); that is,

$$u^*(\tau) = \alpha_1 x_1(\tau) + \alpha_2 x_2(\tau) + \alpha_3, \quad 0 \le \tau \le 1 \tag{41}$$

where $(\alpha_1, \alpha_2, \alpha_3)$ are parameters to be determined from the end-point constraints. This form of u^* can be exploited in two ways: a) the system of differential equations (21) with the control Eq. (41), and constraints, Eq. (22), can be integrated in terms of elliptic integrals of the first and second kind resulting in three transcendental equations to be solved for $(\alpha_1, \alpha_2, \alpha_3)$. The details of this analysis can be found in Sec. IV of Ref. 9. 2) alternatively, a parameter optimization problem can be formulated by applying standard minimization techniques to the end-point function

$$F(\alpha) = q[x_1^2(1;\alpha) + x_2^2(1;\alpha)] + \sin^2[(x_3(1;\alpha) - |w(T) - \pi)/2] \tag{42}$$

where q is a weighting constant and $x_i(1;\alpha)$ denotes the value of state $x_i(\tau)$ at time $\tau = 1$, relative to the parameter vector $\alpha = (\alpha_1, \alpha_2, \alpha_3)$. Further details of this aspect of the problem can be found in Sec. V of Ref. 9.

Computer simulation results are given in Figs. 3 and 4 comparing the piecewise constant controls of Sec. (A) with the minimum energy control, Eq. (41), obtained by minimizing Eq. (42) with $q = 10$ via a Davidon-Fletcher-Powell algorithm. A significant saving in control effort is evident for the initial data close to the unit circle, Fig. 4, when the minimum energy control, Eq. (41), is used in comparison with the piecewise constant control. The differences are much less significant for initial conditions closer to the origin in the (x_1, x_2) plane, as typified in Fig. 3. However, the computational requirements for the minimum energy control, Eq. (41), are significantly more demanding than those for the piecewise constant controls. Further comparative details can be found in Ref. 9.

V. Simulation Results of the Closed Loop Controller

The least squares estimation of Sec. III and the terminal control solutions of subsections A and B of Sec. IV were

Table 1 Actual wind profiles for the simulations

Figure	$w_1(t)$	$w_2(t)$	$\|w(t)\|$	$\angle w(T)$	Δw_1	Δw_2
5	10	$-5+0.01t$	$\sqrt{125-0.1t+10^{-4}t^2}$	$\tan^{-1}\frac{-5+0.01t}{10}$	0	0
6	$10e^{-0.01t}(\cos 0.01t-\sin 0.01t)$	$-10e^{-0.01t}(\cos 0.01t+\sin 0.01t)$	$14.14e^{-0.01t}$	$-45°-0.573°t$	0	0
7	$10e^{-0.01t}$	$-5e^{-0.01t}$	$11.18e^{-0.01t}$	$-26.56°$	-2.0	-2.0
8	$10e^{-0.01t}(\cos 0.01t-\sin 0.01t)$	$-10e^{-0.01t}(\cos 0.01t+\sin 0.01t)$	$14.14e^{-0.01t}$	$-45°-0.573°t$	1.0	1.0

combined for the step-by-step control-estimation sequence as outlined in Sec. II. Simulation studies were carried out for the system, Eq. (1), using a variety of initial conditions $[p_1(0), p_2(0), \theta(0)]$ and wind profiles $[w_1(t), w_2(t)]$ over the total time interval $0 \le t \le 307.5$ sec. The speed of the parachute relative to wind was fixed at $a = 30$ fps. Five subintervals were used for the step-by-step estimation-control sequence with the lengths of these sub-intervals defined by: $t_1 = 7.5$, $t_2 = 82.5$, $t_3 = 157.5$, $t_4 = 232.5$, $T = 307.5$. A small control effort of magnitude 0.01 was exerted over the first subinterval in order to avoid the degeneracy discussed near the end of Sec. III in estimating the parachute heading θ_0. A linear time varying wind model was used in the wind estimation subroutine [Eq. (4) with $n = 1$]:

$$w_1(t) = \alpha_0 + \alpha_1 t, \qquad w_2(t) = \beta_0 + \beta_1 t$$

The actual winds used in the study are given in Table 1. The analytical expressions for both polar and rectangular coordinates of the wind vector are indicated. A step-type disturbance was introduced for some of the runs as indicated by the Δw_i columns in Table 1. These disturbances (where indicated) were imposed at the end of each subinterval according to the rule:

$$w_i(\text{new}) = w_i(\text{old}) + \Delta w_i, \qquad i = 1,2$$

The parachute trajectories under closed loop control are shown in Figs. 5-8 with corresponding plots for the wind profile and the parachute bank angle. Two different trajectories are shown on each figure corresponding to the two different sets of initial conditions indicated. The terminal error, $\|p(T)\|$, is the Euclidean distance in feet, while $\Delta\theta(T)$ denotes the error in the desired parachute heading at the terminal time. These trajectories and data indicate that good terminal accuracy can be obtained for smooth variable winds, with some deterioriation in accuracy for abruptly shifting winds. The bank angles for the most part are quite reasonable, although there were brief moments where bank angles in excess of 30° were called for by the control algorithm. There was no attempt to determine the best sizing of subintervals, nor to experiment with variations in the estimation scheme. Such experimentation is necessary if a practical implementation of this approach is undertaken.

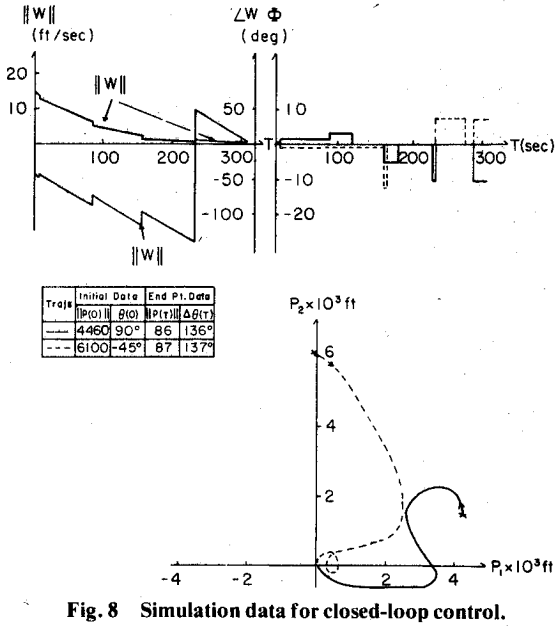

Fig. 8 Simulation data for closed-loop control.

Conclusions

Separating the wind and initial heading estimation problems from the control problem to obtain a step-by-step estimation and control sequence may be a feasible approach to the gliding parachute control problem in a nonuniform wind. Additional experimentation is needed to determine the number and sizing of subintervals, whether or not to combine wind estimates over adjacent subintervals by averaging the estimates over several subintervals, and what form of wind model to use in the estimation scheme. The control aspect of the problem is fairly straightforward from a computational viewpoint, but actuator dynamics have been neglected as indicated by the instantaneous step changes allowed in the parachute bank angle. More sophisticated estimation and control algorithms might offer better performance, but at the expense of more complex computations.

Acknowledgment

This research was supported in part by the U.S. Army Natick Research and Development Command under Contract DAAG-17-73-C-0172. Appreciation is extended to A. L. Murphy Jr. and E. W. Ross of the Natick Laboratories for their help in carrying out this study.

References

[1]Murphy, M. B. and Corlis, N. E., "Para-Foil Electronic Guidance System," Sandia Labs., Albuquerque, N. Mex., Tech. Rept. SC-DR-710279, July 1971.

[2]Slayman, R. A., Bair, H. W. and Rathburn, T. W., "500 Pound Controlled Airdrop Cargo System," Goodyear Aerospace Corp., Akron, Ohio, GER-13801, Sept. 1970.

[3]Knapp, C. E. and Barton, W. R., "Controlled Recovery of Payloads at Large Glide Distances Using the Para-Foil," *Journal of Aircraft*, Vol. 5, March-April 1968, pp. 112-118.

[4]Goodrick, T. F., "Wind Effect on Gliding Parachute Systems with Non-Proportional Automatic Homing Control," U. S. Army Natick Labs., Natick, Mass., Rept. TR-70-28-AD, Nov. 1969.

[5]Murphy, A. L. Jr., "Trajectory Analysis of a Radial Homing Gliding Parachute in a Uniform Wind," U.S. Army Natick Labs. Report 73-2-AD, Sept. 1971.

[6]Murphy, A. L., Jr., "Azimuth Homing in a Planar Uniform Wind," U.S. Army Natick Labs., Rept. 74-42-AD, April 1973.

[7]Goodrick, T. F., Pearson, A. E. and Murphy, A. L., Jr., "Analysis of Various Automatic Homing Techniques for Gliding Airdrop Systems With Comparative Performance in Adverse Winds," AIAA Paper 73-462, Palm Springs, Calif., 1973.

[8]Wei, K. C. and Pearson, A. E., "Numerical Solution to the Optimal Control of a Gliding Parachute System," U.S. Army Natick Labs. Rept. 75-107-AMEL, Oct. 1974.

[9]Koopersmith, R.M. and Pearson, A. E., "Determination of Trajectories for a Gliding Parachute System," U.S. Army Natick Labs. Rept. 75-117 AMEL, April 1975.

[10]Pearson, A. E., "Optimal Control of a Gliding Parachute System," U.S. Army Natick Labs. Rept. 73-30-AD, Aug. 1972.

[11]Pearson, A. E. and Wei, K. C., "Control of a Gliding Parachute System in a Nonuniform Wind," U.S. Army Natick Labs. Rept. 76-60 AMEL, May 1976.